SYNTHESIS AND CHARACTERIZATION OF NANOCOMPOSITE NiFe$_2$O$_4$@SalenSi AND ITS APPLICATION IN EFFICIENT REMOVAL OF Ni(II) FROM AQUEOUS SOLUTION

Narjes Babadi[1], Haman Tavakkoli[1*] and Mozhgan Afshari[2]

[1]Department of Chemistry, Ahvaz Branch, Islamic Azad University, Ahvaz, Iran
[2]Department of Chemistry, Shushtar Branch, Islamic Azad University, Shushtar, Iran

ABSTRACT. In this work, nano ferrite spinel NiFe$_2$O$_4$ was synthesized by sol-gel method and characterized by SEM, XRD, FT-IR, and VSM. In second step Schiff base made from salicylaldehyde and amino propyl triethoxy silane was used for modification of the synthesized nano ferrit. In the third step removal of Ni(II) was done using modified adsorbent and 95% efficiency was achieved. The removal rate was determined by atomic absorption spectroscopy. These studies showed that the Freundlich isotherm model was fitted well with adsorption data. Moreover, the pseudo-second order kinetic model was fitted very well with experimental data. The results demonstrated that NiFe$_2$O$_4$@SalenSi nanoadsorbent can be used for the removal and recovery of metal ions from wastewater over a number of cycles, indicating its suitability for the design of a continuous process.

KEY WORDS: Nano ferrite, Sol-gel method, Schiff base, Removal of Ni(II), Magnetic nanocomposite

INTRODUCTION

The scarcity of water in terms of both quantity and quality has become a significant threat to the well-being of humanity. In particular, the quality of drinking water has become a serious concern, with the rapid escalation of industrialization towards a developed society. The waste products generated from the textiles, chemicals, mining and metallurgical industries are mainly responsible for contaminating the water [1]. This contaminated water contains non-biodegradable effluents, such as heavy metal ions (arsenic, zinc, copper, nickel, mercury, cadmium, lead and chromium, etc.) and organic materials that are carcinogenic to human beings and harmful to the environment [2]. According to the WHO, the limit of the toxicity value for nickel is 130 μg/L, assuming a 60 kg adult, drinking two liters of water per day. However, the presence of nickel at higher levels in the human body can cause serious lung and kidney problems as well as gastrointestinal distress, pulmonary fibrosis and skin dermatitis [3].

Several conventional methodologies such as precipitation [4], ion exchange [5], filtration membrane technology [6], electrochemical processes [7] and adsorption process [8] are available for heavy metal removal and other pollutants from wastewaters. Generally, they are expensive or ineffective sometimes, especially when the metal concentration is higher than 100 mg/L [9]. Among all the treatments proposed, adsorption using sorbents is one of the most popular methods. It is now recognized as an effective, efficient and economic method for water decontamination applications and for separation for pilot purpose.

Some nanoadsorbents can be easily recovered or manipulated with an external magnetic field and show a good capacity for the rapid and efficient adsorption of multivalent metal cations from aqueous solutions. Composite microspheres can be applied to remove heavy metal ions from industrial wastewater because the surface of the microspheres is covered with SiO$_2$, and the SiO$_2$ is inactive and can adsorb heavy metal ions (such as Hg^{2+} and Pb^{2+}) [10], or using supplementary material modification process magnetic nano particles, for example: capped by thiol [11], capped by amine [12] or capped by Schiff base [13]. The use of monodisperse amine-

_____

terminated $Fe_3O_4@SiO_2–NH_2$ for the removal of metal ions was recently reported. These amine-terminated core-shell magnetic nanoparticles show effective removal of Pb^{2+} [14] and removal heavy metals hybrid composite such as: $Fe_3O_4–SiO_2$-poly(1,2-diaminobenzene) [15], amine-$Fe_3O_4@SiO_2@meso-SiO_2$ [16] and EDTA-γ-$Fe_3O_4@SiO_2$/Thiol-γ-$Fe_3O_4@SiO_2$ [17]. The effective removal of heavy metal ions from an aqueous solution using modified magnetic nanoparticles by polymer [18] for example polypyrrole [19] has been developed by the covalent binding of poly(acrylic acid) on the surface of Fe_3O_4 nanoparticles followed by sulfonation using sulfanilic acid via carbodiimide activation [20] capped by EDA polymers [21]. Amine-functionalized magnetite chitosan nanocomposites as a recyclable tool was used for the removal of heavy metals (amine-$Fe_3O_4@SiO_2$) [22], magnetic nanoparticles surface modification using acids such as humic acid (humic acid-Fe_3O_4) [11] and ascorbic acid (ascorbic acid-Fe_3O_4) [23]. Also to remove heavy metals by magnetic nanoparticles surface modification using some chemicals such as DMSA (DMSA-Fe_3O_4) [24]. There is recent research from composite to remove heavy metal ions from aqueous solutions used. The optimum conditions for this research pH 6, 24 h as well as the reaction efficiency100% (Cu^{2+}, Pb^{2+}, Hg^{2+}, As^{3+}), 40% (Co^{2+}), 22% (Cd^{2+}) and 25% (Ni^{2+}) [25, 26].

In this work, nano ferrite spinel $NiFe_2O_4$ was synthesized. In second step Schiff base made from salicylaldehyde and amino propyl triethoxysilane was used for modification of synthesized nano ferrit, also the characterization of such new phases and their capabilities toward Ni(II) removal were done, respectively. Therefore, in the batch system the effects of pH, adsorbent dosage, initial concentration and contact time on the adsorption capacity were investigated.

EXPERIMENTAL

Reagents

$Ni(NO_3)_2.6H_2O$ (99.99% purity) and $Fe(NO_3)_3.9H_2O$ (99.99% purity) were obtained from Merck, Germany; citric acid (CA) (99.5% purity) was purchased from Aldrich, USA. NaOH (99.99% purity), HCl (37.00% purity), CH_3OH (99.99% purity), C_2H_5OH (99.99% purity), salicylaldehyde ($C_7O_2H_7$), 3-amino propyl triethoxysilane ($C_6H_6O_3NH_2Si$) were provided by Merck. All the reagents were of analytical grade and thus used as received. Also deionized water was used throughout the experiments.

Preparation of NiFe₂O₄

The nickel ferrite was synthesized by sol-gel method. First the aqueous solution of metal nitrate with nominal atomic ratios Fe:Ni = 2:1 was mixed together in deionized water. Citric acid (CA) was proportionally added to the metal ion solution to gain the same amounts of equivalents. The solution was concentrated by evaporation at approximately 50 ^{o}C with simultaneous stirring for 1 h to convert it to stable (Fe, Ni)/CA complex. The solution was heated (while being stirred) at approximately 75 ^{o}C to remove excess water. Then the dry gel was obtained by letting the sol into an oven heating it slowly up to 110 ^{o}C and keeping it for 6 h in a baking oven. The gel pieces were grounded in an agate mortar to form fine powder. Finally $NiFe_2O_4$ nanoferrite was obtained.

Preparation of the Schiff base

The Schiff base was synthesized according to the literature [27]. A solution of salicylaldehyde (4 mmol) in CH_3CN or CH_3OH (20 mL) was treated with amino propyl triethoxysilane in a molar ratio of 1:1.5. The reaction mixture was refluxed for four hours. The result was a pale yellow Schiff base that is shown in (Scheme 1).
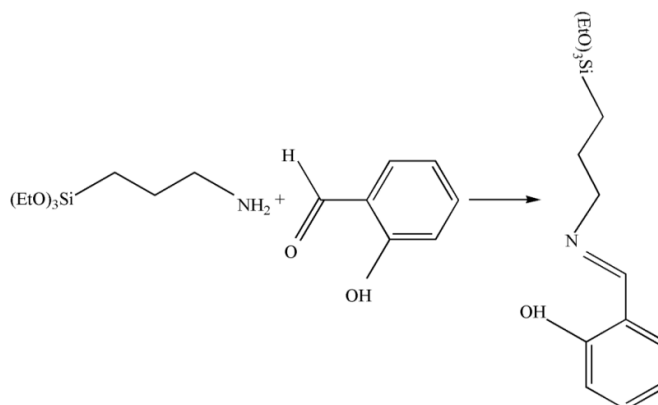
Scheme 1. Preparation process of Schiff base bonding to nickel ferrite.

Preparation of nano composites NiFe₂O₄@SalenSi

At this stage nickel ferrite (1 mmol) was added to the solution. Then the reaction mixture was refluxed for twenty-four hours. The solid residue was filtered and washed with CH_3OH (8 drops) and chloroform (3 drops). After that it was laid in the desiccators for a few hours in order to be dried, shown in (Figure 1).
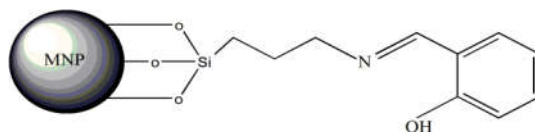
Figure 1. An illustration for NiFe₂O₄@SalenSi nanoadsorbents.

Adsorbent characterization

Several techniques were employed to analyze and validate the synthesized powder. For structural investigation of calcinated powder at 700 °C, powder X-ray diffraction (XRD) measurements were carried out in the region of (2θ = 20 to 70°) using CuK_α radiation on a Rigaku D/MAX RB XRD diffract meter equipped with a curved graphite monochromator. To study the surface morphology scanning electron microscopy (SEM) images were carried out. The complex polymeric gel and derived powders have been also analyzed by Fourier transform infrared spectroscopy (FTIR) on Perkin Elmer BX II FTIR spectrometer. The magnetic properties (M-H curve) were evaluated on a BHV-55 vibrating sample magnetometer (VSM). This analysis was measured at room temperature using the magnetic field 1000 Oe to -1000 Oe. Finally with the help of atomic absorption spectroscopy AAS final concentration of nickel ions was achieved.

Ni(II) removal experiments

A prepared solution of Ni(II) was distributed into different flasks (1 L capacity) and pH was adjusted with the help of the pH meter (HORIBA F 11 E, Japan made). The initial pH value of the soluble metal ion was adjusted to the desired levels, using either HCl (0.5 M) or NaOH (0.5 M). A known mass of NiFe₂O₄@SalenSi powder (adsorbent dosage) was then added to 20 mL

of soluble [Ni(II)], and the obtained suspension was immediately stirred for a predefined time. All experiments were done at room temperature. The investigated ranges of the experimental variables were as follows: concentrations of pollutants (10-50 mg/L), pH of solution (2-11), adsorbent dosage (0.02, 0.03 and 0.04 g) and mixing time (30-120 min).

Adsorption capacity and removal efficiency were calculated according to the following equations [28]:

$$\text{Removal rate} \ \% = \frac{C_o - C(e)}{C_o} \times 100 \tag{1}$$

where qe (mg/g) is adsorption capacity; E (%) is removal efficiency; C_0 (mg/L), and C_e (mg/L) are initial and equilibrated adsorbate concentrations, respectively;

Reusability of nanoadsorbents

To test the reusability of the nanoadsorbents, the $NiFe_2O_4$@SalenSi nanoadsorbents containing Ni(II) were washed with CH_3OH. After that $NiFe_2O_4$@SalenSi nanoadsorbents were thoroughly washed with deionized water till. Then, the washed nanoadsorbents were at 150 ^{o}C for 15 min and reused for the subsequent adsorption cycle. Five cycles of consecutive adsorption–desorption–regeneration were carried out to validate the reusability of $NiFe_2O_4$@SalenSi nanoadsorbents for the removal and recovery of Ni(II).

RESULTS AND DISCUSSION

X-Ray diffraction

XRD patterns of the synthesized powder which was calcinated at temperature 700 ^{o}C for 9 h (heating rate: 3 ^{o}C/min) is shown in (Figure 2). XRD results reveal the existence of nano ferrite for sol-gel method. When the precursor was calcinated at 700 ^{o}C for 9 hours, several sharp peaks were observed attributed to the nano ferrite $NiFe_2O_4$ by comparison with standard XRD spectra. The diffraction peaks at 2θ angels appeared in the order of 30.27^o, 35.75^o, 43.33^o, 43.56^o, 57.4^o and 62.9^o can be assigned to scattering from the (2 2 0), (3 1 1), (4 0 0), (5 1 1) and (4 4 0) planes of the nano ferrite $NiFe_2O_4$ type crystal lattice, respectively. XRD data shows $NiFe_2O_4$ crystallizes in a hexagonal phase with (a = b = 4.866, c = 12.652) and space group $R^{-3}m$ (166). The crystallite sizes were calculated using XRD peak broadening of the (311) peak using the Scherer's formula:

$$D_{hkl} = \frac{0.9\,\lambda}{\beta_{hkl} \cos\theta_{hkl}} \tag{2}$$

where D_{hkl} is the particle size perpendicular to the normal line of (hkl) plane, β_{hkl} is the full width at half maximum, θ_{hkl} is the Bragg angle of (hkl) peak, and λ is the wavelength of X-ray. The particle size of nanoparticles calcinated at 700 ^{o}C is about 52.75 nm.

SEM analysis

Scanning electron microscopy (SEM) of nanoferrite prepared by the sol-gel method and modified by Schiff base is shown in Figure 3 (a, b). (a): This image, exhibit typical morphology for prepared nanopowders ($NiFe_2O_4$) with uniform particles distribution and regular shapes. (b): The micrograph represents formation of agglomerated particles with Schiff base addition. However, appearance of bigger particles on the surface seems to be dominant.
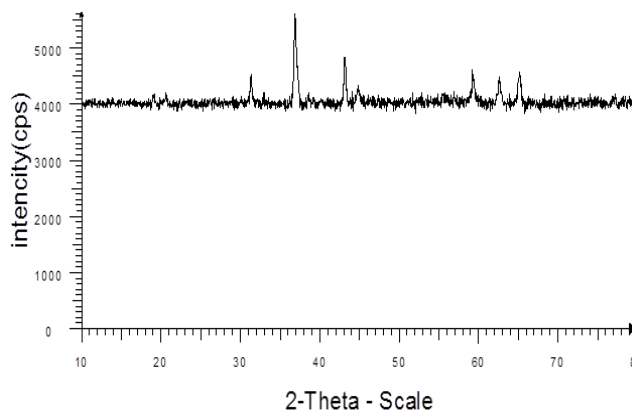
Figure 2. XRD patterns of samples of the NiFe$_2$O$_4$ nanopowder calcinated at 700 $^{\circ}$C.
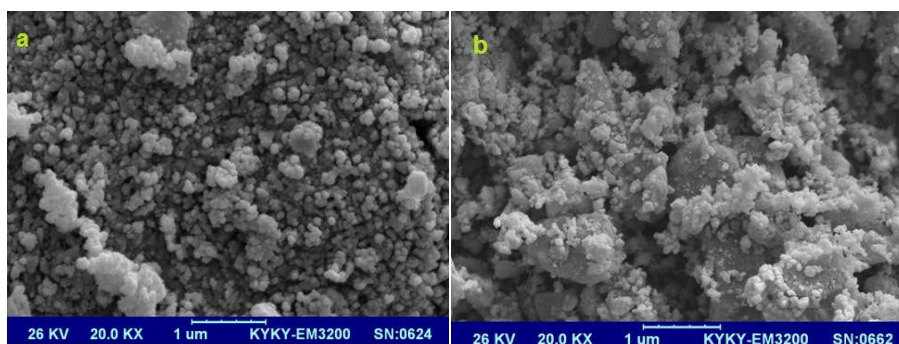

Figure 3. (a) SEM images of the NiFe$_2$O$_4$nanopowders and (b) SEM images of the NiFe$_2$O$_4$@SalenSi nanoadsorbents.

FT-IR spectroscopy

The FT-IR spectra of the NiFe$_2$O$_4$ fresh xerogel and calcinated xerogel and NiFe$_2$O$_4$@SalenSi in the range of 500-4000 cm^{-1} are shown in Figure 4 (a, b, c). The dried gel of the sample shows the characteristic peaks at about 1778.17, 1643.81 and 1427.58 cm^{-1}, which correspond to the symmetric and anti-symmetric stretching mode of carboxylate group [29, 30]. The peak around 1027.55 cm^{-1} is attributed to C–O bond [31]. As seen in (Figure 4), the bands correspond to O–H group, NO$_3$, and carboxylate ligand disappears as the gel which was calcinated at 700 $^{\circ}$C. This indicates the possibility of metal carboxylate dissociation and conversion to metal oxides during the calcination process. Also, the observed peak at about 607.20 cm^{-1} is due to the stretching internal vibrations of octahedral oxygen in nickel ferrite oxide structure.

In the FT-IR spectrum Schiff base nickel ferrite nanoparticles deposited on the surface, Figure 4 (c), the broad peak in 1200-1000 cm^{-1} belongs to Si-O-Si stretching vibration. In addition, a peak at 1652 cm^{-1} observed is attributed to the stretching vibration of C=N bond.
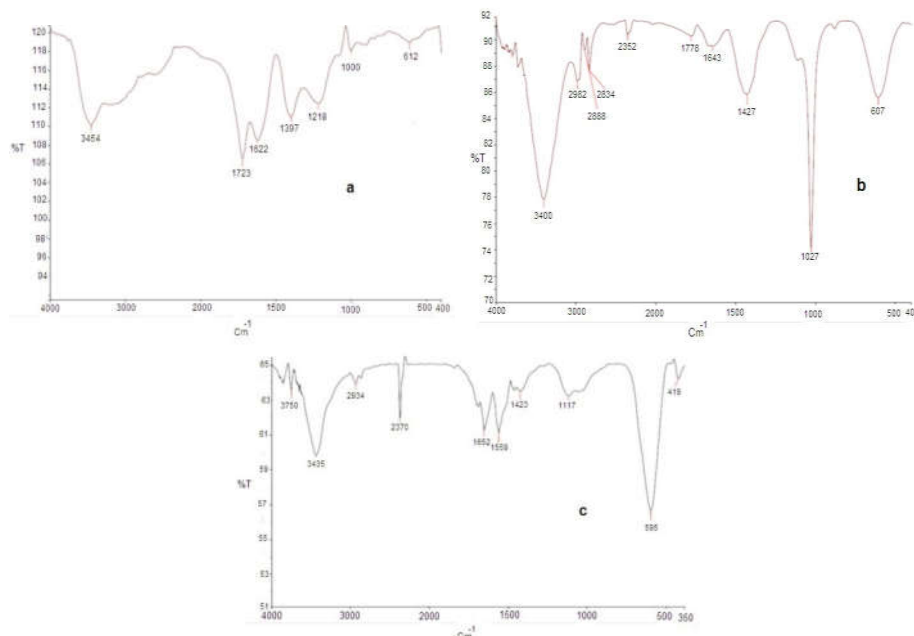
Figure 4. FT-IR spectra of $NiFe_2O_4$ nanopowders (a) and the calcinated powders at 700 ^{o}C (b), and spectra of $NiFe_2O_4$@SalenSi nano adsorbents (c).

Vibrating sample magnetometer (VSM) analyses

Ferromagnetism properties of the $NiFe_2O_4$ at room temperature are shown in Figure 5 (a, b). (a) The saturation magnetization (M_s) is 9.87 emu/g. The high M_s and low remnant magnetization (M_r = 43.616 emu/g) means that $NiFe_2O_4$ can be separated easily from solution under an external magnetic field and distribute well in reused cycles, which is favorable for reusing of the adsorbent. (b) Ferromagnetism properties of the $NiFe_2O_4$@SalenSi also include the saturation magnetization (Ms) of 10.42 emu/g. The high M_s and low remnant magnetization (M_r = 54.125 emu/g).

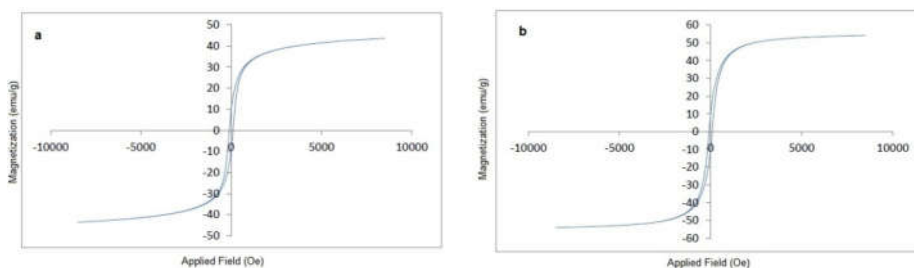Figure 5. VSM   spectra   of $NiFe_2O_4$nanopowders   (a)   and   VSM   spectra   of $NiFe_2O_4$@SalenSinanoadsorbents (b).

Adsorption study

Effect of pH

The solution pH is an important parameter that affects the adsorption of Ni(II). The effect of the initial solution pH on the metals removal efficiency of Ni(II) by $NiFe_2O_4$@SalenSi nanoparticles

was evaluated at different pH values, ranging from 2 to 11, with a stirring time of 45 min. The initial concentrations of Ni(II) and adsorbent dosage were set at 10 mg/L and 15.0 mg/L, respectively. As shown in Figure 6, pH 9 seems to lead to the best result; so this pH was selected to run further experiments.
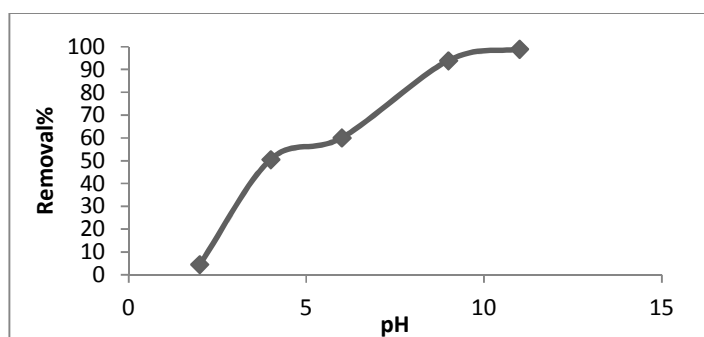

Figure 6. Effect of pH on Ni(II) adsorption onto NiFe$_2$O$_4$@SalenSi nanoadsorbents. (Initial Ni(II) concentration 10 mg/L, adsorbent dose 15.0 mg/L, shaking rate: 200 rpm, contact time: 45 min).

Effect of contact time and adsorbent dosage

To further assessing of Ni(II) removal, the effects of contact time and adsorbent concentration on the removal of Ni(II) by NiFe$_2$O$_4$@SalenSi nanoparticles were examined. Ni(II) concentrations and pH of the solutions were fixed at 10 mg/L and 9 respectively for all batch experiments. Results are shown in. Figure7. As indicated, increasing of contact time in different dosages of adsorbent led to decrease the concentration of Ni(II). This behavior was also observed when the adsorbent dosage increased from 10.0 and 15.0 to 20.0 mg/L. This decreasing in the concentration is due to the adsorption of Ni(II) on NiFe$_2$O$_4$@SalenSi nanoparticles and the greater number of adsorption sites for Ni(II) made available at greater NiFe$_2$O$_4$@SalenSi dosages. The removal efficiency of Ni(II) at the initial dosage of 15.0 mg/L, and 45 min by keeping constant stirring was attained about 94.6%.
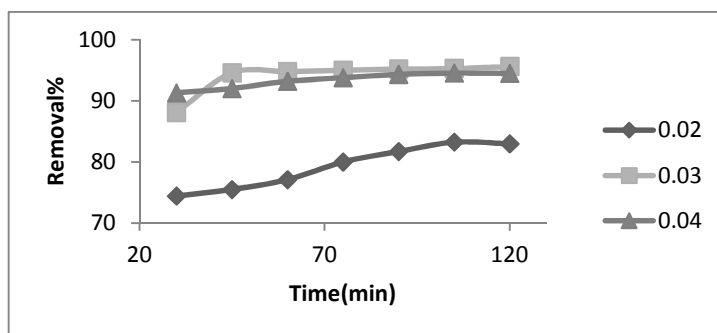

Figure 7. Effect of contact time on the removal of Ni(II) at different initial. (Initial Ni(II) concentrations: 10 mg/L, shaking rate: 200 rpm, initial pH: 9).
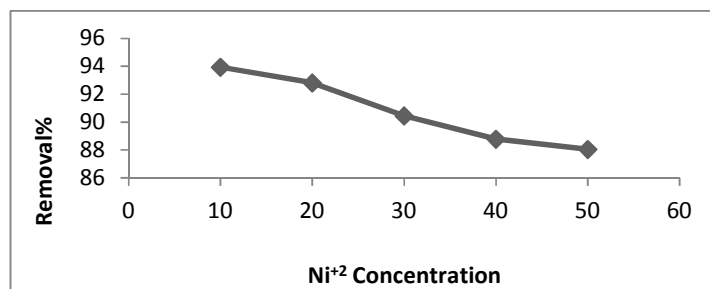
Figure 8. Effect of initial metal ion concentration on removal of Ni(II). (Initial pH: 9, adsorbent
dose 15.0 mg/L, shaking rate: 200 rpm, contact time: 45 min).

Effect of Ni(II) concentration

The Ni(II) concentration is another important parameter that can affect the adsorption process. The effect of initial Ni(II) concentration on metal removal efficiency by NiFe$_2$O$_4$@SalenSi particles was studied by varying the initial Ni(II) concentration from 10 to 50 mg/L at pH 9, a nanoadsorbent dosage of 15.0 mg/L and contact time of 45 min, as shown in Figure 8. Results verify that metal removal of Ni(II) decreases with increasing the initial concentration. Obviously, the percentage removal of Ni(II)was around 94.6% at a concentration of 10 mg/L .

Reusability of nano adsorbent NiFe$_2$O$_4$@SalenSi

Figure 9 shows the removal efficiency, R (%), of Ni(II), during five cycles of adsorption–desorption–regeneration, from a 20 mL solution of initial Ni(II) concentration 10 mg/Lat pH 9. As can be seen, no significant decrease in the adsorption capacity of NiFe$_2$O$_4$@SalenSi nanoadsorbent during the five cycles was observed. The results demonstrated that NiFe$_2$O$_4$@SalenSi nanoadsorbent can be used for the removal and recovery of metal ions from wastewater over a number of cycles, indicating its suitability for the design of a continuous process. It is noteworthy that commercially available adsorbents such as activated carbon are costly, time-consuming and their regeneration is essential. Actually, the regeneration and recovery of spent activated carbons is the most expensive part of the adsorption technology and it accounts for about 75% of the total operating and maintenance costs [32]. However, it seems that this is not the case for the regeneration of spent NiFe$_2$O$_4$@SalenSi nanoadsorbents. Therefore, NiFe$_2$O$_4$@SalenSi nanoadsorbent is a cost-effective alternative with fast adsorption rate and its regeneration is simple and may be not necessary, especially for in situ applications [33].

Adsorption kinetic studies

The kinetic studies describe that the solute uptake rate for choosing optimum operating conditions for designing purposes. In order to investigate the mechanism of adsorption and potential rate controlling steps such as chemical reaction, diffusion control and mass transport process, kinetic models have been used to test experimental data from the adsorption of Ni(II). These kinetic models were analyzed using pseudo-first-order and pseudo-second-order which were respectively presented as follows in Eqs.

$$\log(q_e - q_t) = \log q_e - \left(\frac{k_1}{2/303}\right) t \tag{3}$$

$$\frac{t}{qt} = \frac{1}{K2q_e} + \frac{1}{q_e} t \tag{4}$$

where t is the contact time of adsorption experiment (min); q$_e$ (mg/g) and q$_t$ (mg/g) are respectively the adsorption capacity at equilibrium and at any time t. The values of the rate constant, k$_1$ and k$_2$ are -0.053 and 0.161 (M^{-1} min^{-1}), respectively.

The adsorption process of Ni(II) can be well fitted by using the pseudo-second order rate. The linear regression coefficient value R^2 (0.999) obtained for pseudo-second-order constant. Kinetics was closer to unity than the R^2 value (0.907) for first-order kinetics. This indicates that the pseudo-second-order kinetic model provided good correlation for the adsorption of Ni(II) ions onto NiFe$_2$O$_4$@SalenSi.
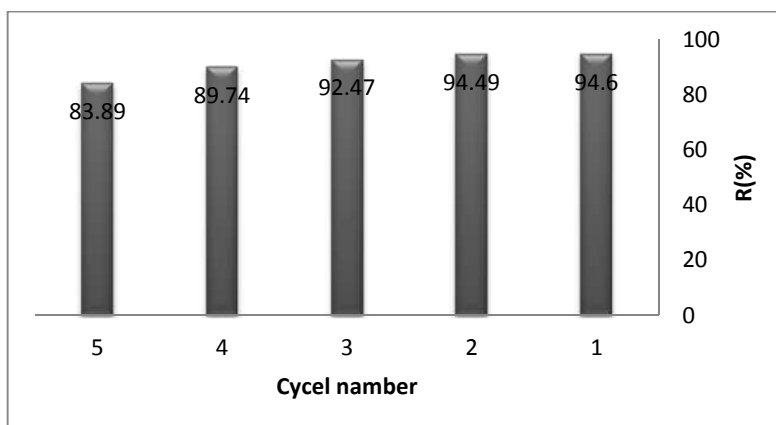

Figure 9. Reusability of NiFe$_2$O$_4$@SalenSi nanoadsorbents for adsorption/desorption of Ni(II) concentration 10 mg/L, adsorbent dose 15.0 mg/L, shaking rate: 200 rpm, contact time: 45 min, initial pH: 9).

Adsorption isotherm studies

Adsorption isotherm studies analysis of the equilibrium data is important to develop an equation which accurately represents the results which could be used for designing purposes. The results obtained for adsorption of Ni(II) ions were analyzed by the use of well-known models given by the Langmuir, Freundlich and Temkin isotherm models. For the sorption isotherms, initial metal ion concentration was varied whereas solution pH and amount of adsorbent were held constant.

$$\frac{C_e}{q_e} = \frac{1}{k_l q_{max}} + \frac{C_e}{q_{max}} \tag{5}$$

$$\log q_e = \log K_F + \frac{1}{n} \log C_e \tag{6}$$

$$q_e = A + B \ln C_e \tag{7}$$

where C$_e$ is the Ni(II) concentration in the solution (mg/L), q$_e$ is the Ni(II) concentration in the solid adsorbent (mg/g), q$_m$ is the maximum adsorption capacity (mg/g), K$_l$ is a constant related to the energy of adsorption (L/g), K$_F$ and n are constants of the Freundlich equation. The constant K$_F$ represents the capacity of the adsorbent for the adsorbate and n is related to the adsorption distribution (mg$^{1-1/n}$ L$^{1/n}$/g), A (L/g) is Temkin constant representing adsorbent–adsorbate interactions and B (mg .L^{-1}) is another constant related with adsorption heat. The R^2 values for

the Freundlich model ($R^2 = 0.999$) are closer to unity than those for the other isotherm models (Langmuir: $R^2 = 0.958$ and Temkin: $R^2 = 0.955$) for adsorption process onto $NiFe_2O_4$@SalenSi. This indicates that the adsorption of Ni(II) on $NiFe_2O_4$@SalenSi particles is better described by the Freundlich model than the Langmuir and Temkin models and generally it has been found better suited for characterizing monolayer adsorption process onto the homogenous adsorbent surface (Figure 10 (a, b, c)) [34].
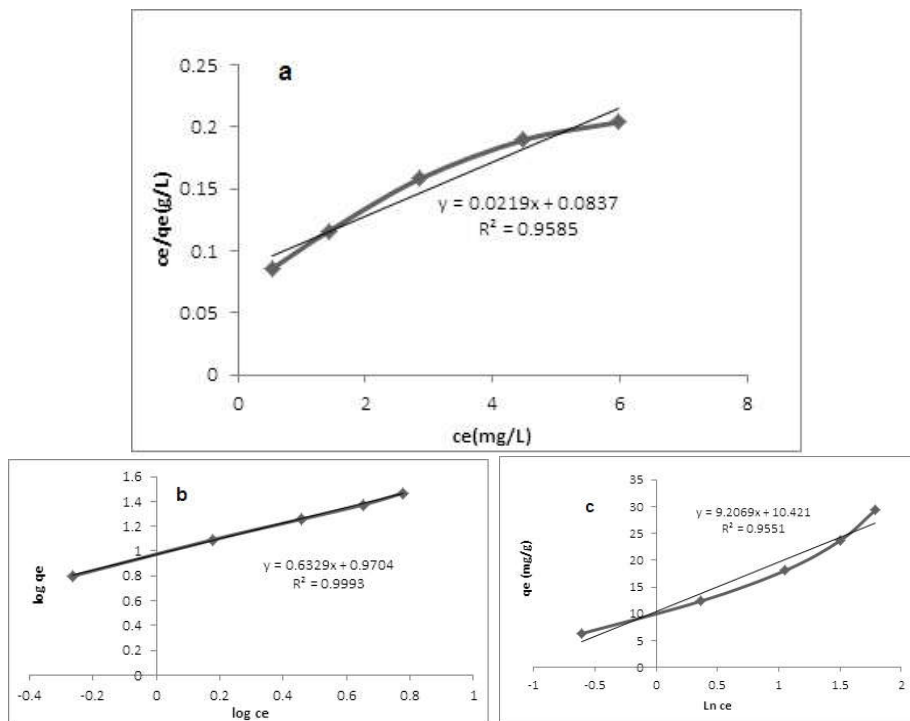

Figure 10. Isotherm plots of Ni(II) adsorption onto $NiFe_2O_4$@SalenSi nanoadsorbents. (Initial Ni(II) concentration 10 mg/L, adsorbent dose 15.0 mg/L, shaking rate: 200 rpm, contact time: 45min, initial pH: 9). a: Langmuir isotherm, b: Freundlich isotherm and c: Temkin isotherm.

CONCLUSION

This study showed that $NiFe_2O_4$@SalenSi nanoadsorbent could be used as an alternate to conventional adsorbents for the removal of metal ions from wastewater in a very short time with high removal efficiency, whereas, single $NiFe_2O_4$ was not be able to removal of metal ions. The removal of Ni(II), as a typical metal ion commonly present in wastewater, by adsorption onto $NiFe_2O_4$@SalenSi nanoadsorbents was successfully accomplished. Adsorption was very rapid and equilibrium was achieved in less than 45 min. Also the adsorption was highly dependent on the initial concentration of Ni(II) and pH. Maximum removal was observed at pH 9. Adsorption increased as the initial concentration of Ni(II). The adsorption isotherms were also determined and were appropriately described by both Langmuir and Freundlich models, with a better fitting to the Freundlich model than the Langmuir model. Therefore, $NiFe_2O_4$@SalenSi nanoadsorbents are recommended as fast, effective and inexpensive adsorbents for rapid removal and recovery

of metal ions from wastewater effluents. The pseudo-second-order kinetic model provided good correlation for the adsorption of Ni(II) ions onto NiFe$_2$O$_4$@SalenSi. The desorption and regeneration studies indicated that nanoadsorbents can be used repeatedly, without impacting the adsorption capacity. Therefore, NiFe$_2$O$_4$@SalenSi nanoadsorbents are recommended as fast, effective and inexpensive adsorbents for rapid removal and recovery of metal ions from wastewater effluents.

REFERENCES

1   Gómez-Álvarez, A.; Valenzuela-García, J.L.; Meza-Figueroa, D.; De, M.; O-Villanueva, L.A.; Ramírez-Hernández, J.; Almendariz-Tapia, J.; Pérez-Segura E. Impact of mining activities on sediments in a semi-arid environment: San Pedro River, Sonora, Mexico. *Appl. J. Geochem*. **2011**, 26, 2101‒2112.

2   Shen, Y.F.; Tang, J.; Nie, Z.H.; Wang, Y.D.; Ren, Y.; Zuo, L. Preparation and application of magnetic Fe$_3$O$_4$ nanoparticles for wastewater purification. *Technol*. **2009**, 68, 312-329.

3   Borba, C.E.; Guirardello, R.; Silva, E.A.; Veit, M.T.; Tavares, C.R.G. Removal of nickel(II) ions from aqueous solution by biosorption in a fixed bed column, experimental and theoretical breakthrough curves. *Biochem Eng*. **2006**, 30, 184-191.

4   Martins, A.; Mata, T.M.; Gallios, G.P.; Vaclavikova, M.; Stefusova, K. Modeling and simulation of heavy metals removal from drinking water by magnetic zeolite. *Water Treatment Technologies for the Removal of High-Toxicity Pollutants*. *Project* **2010**; No. APVT 51, 017104, 61-84. Available at: https://link.springer.com/book/10.1007/978-90-481-3497-7.

5   Yuan, P.; Liu, D.; Fan, M.; Yang, D.; Zhu, R.; Ge, F.; Zhu, J.X.; He, H. Removal of hexavalent chromium [Cr(VI)] from aqueous solutions by the diatomite supported/unsupported magnetite nanoparticles. *J. Hazard Mater*. **2010**, 173, 614-621.

6   Song, J.; Oh, H.; Kong, H.; Jang, J. Polyrhodanine modified anodic aluminum oxide membrane for heavy metal ions removal. *J. Hazard. Mater*. **2011**, 187, 311-317.

7   Karami, H. Heavy metal removal from water by magnetite nanorods. *J. Chem. Eng*. **2013**, 219, 209-216.

8   Chiban, M.; Soudani, A.; Sinan, F.; Persin, M. Single, binary and multi-component adsorption of some anions and heavy metals on environmentally friendly *Carpobrotus edulis* plant. *Colloids Surf. B* **2011**, B 82, 267-276.

9   Miretzky, P.; Saralegui, A.; Cirelli, A.F. Simultaneous heavy metal removal mechanism by dead macrophytes. *Chemosphere* **2006**, 62, 247-254.

10 Haibo, Hu.; Zhenghua, W.; Ling, P. Synthesis of monodisperse Fe$_3$O$_4$@silica core–shell microspheres and their application for removal of heavy metal ions from water. *J. Alloy Compd*. **2010**, 492, 656-661.

11 Hakami, O.; Zhang Y.; Banks, C.J. Thiol functionalized mesoporous silica-coated magnetite nanoparticles for high efficiency removal and recovery of Hg from water. *Water Res*. **2012**, 46, 3913-3922.

12 Zhenxin, Z.; Fengwei, Z.; Qianqian, Z.; Wei, Z.; Baochun, M.; Yong, D. Magnetically separable polyoxometalate catalyst for the oxidation of dibenzothiophene with H$_2$O$_2$. *J. Colloid Interface Sci*. **2011**, 360, 189-194.

13 Bagheri, H.; Afkhami, A.; Saber-Tehrani, M.; Khoshsafar, H. Preparation and characterization of magnetic nanocomposite of Schiff base/silica/magnetite as a preconcentration phase for the trace determination of heavy metal ions in water, food and biological samples using atomic absorption spectrometry. *Talanta* **2012**, 97, 87-95.

14 Zhang, J.; Zhai, S.; Li, S.; Xiao, Z.; Song, Y.; Ana, Q.; Tian, G. Pb(II) removal of Fe$_3$O$_4$@SiO$_2$–NH$_2$ core–shell nanomaterials prepared via a controllable sol–gel process. *J. Chem. Eng*. **2013**, 215, 461-471.

15 Zhang, F.; Lan, J.; Zhao, Z.; Yang, Y.; Tan, R.; Song, W. Removal of heavy metal ions from aqueous solution using Fe_3O_4–SiO_2-poly(1,2-diaminobenzene) core–shell sub-micron particles. *Colloid Interface Sci*. **2012**, 387, 205-212.

16 Yuan, Q.; Li, N.; Chi, Y.; Geng, W.; Yan, W.; Zhao, Y.; Li, X.; Dong, B. Effect of large pore size of multifunctional mesoporous microsphere on removal of heavy metal ions. *J. Hazard. Mater*. **2013**, 254, 157-165.

17 Sinha, A.; Jana, N.R. Functional, mesoporous, superparamagnetic colloidal sorbents for efficient removal of toxic metals. *Chem. Commun*. **2012**, 48, 9272-9274.

18 Ge, F.; Li, M.M.; Ye, H.; Zhao, B.X. Effective removal of heavy metal ions Cd^{2+}, Zn^{2+}, Pb^{2+}, Cu^{2+} from aqueous solution by polymer modified magnetic nanoparticles. *J. Hazard. Mater*. **2012**, 211, 366-372.

19 Zhang, H.; Zhong, X.; Jing-Juan, X.u.; Chen, H.Y. Fe_3O_4/Polypyrrole/Au nanocomposites with core/shell/shell structure: Synthesis, characterization, and their electrochemical properties. *Langmuir* **2008**, 24, 13748-13752.

20 Sou-Yee, M.; Dong-Hwang, C. Binding and sulfonation of poly(acrylic acid) oniron oxide nanoparticles: A novel, magnetic, strong acid cation nano-adsorbent. *Macromol. Rapid Commun*. **2005**, 26, 1567-1571.

21 Zhao, Y.G.; Shen, H.Y.; Pan, S.D.; Hu, M.Q. Synthesis, characterization and properties of ethylenediamine-functionalized Fe_3O_4 magnetic polymers for removal of Cr(VI) in wastewater. *J. Hazard. Mater*. **2010**, 182, 295-302.

22 Liu, X.; Hu, Q.; Fang, Z.; Zhang X.; Zhang, B. Magnetic chitosan nanocomposites: A useful recyclabletool for heavy metal ion removal. *Langmuir*. **2009**, 25, 3-8.

23 Feng, L.; Cao, M.; Ma, X.; Zhu Y.; Hu, C. Superparamagnetic high-surface-area Fe_3O_4 nanoparticles as adsorbents for arsenic removal. *J. Hazard. Mater*. **2012**, 217, 439-446.

24 Singh, S.; Barick K.C.; Bahadur, D. Surfaceengineered magnetic nanoparticles for removal of toxic metal ions and bacterial pathogens. *J. Hazard. Mater*. **2011**, 192, 1539-1547.

25 Singh, S.; Barick K.C.; Bahadur, D. Fe_3O_4 embedded ZnO nanocomposites for the removal of toxic metal ions, organic dyes and bacterial pathogens. *J. Mater. Chem*. **2013**, A1, 3325-3333.

26 Elhami, S.; Sharifi, M. Development of an efficient procedure for the preconcentration of copper(II) after solid phase extraction on modified sawdust. *Bull. Chem. Soc. Ethiop*. **2014**, 28, 321-328.

27 Tabatabaee, M.; Heravi, M.M.; Sharif, M.; Esfandiyari, F. Fast and efficient method for imination of n-aminorhodanine using inorganic solid support under microwave irradiation and classical heating. *E. J. Chem*. **2011**, 8, 535-540.

28 Ren, Y.M.; Wei, X.; Zhang, M.L. Synthesis and adsorption properties of sponge like porous $MnFe_2O_4$. *J. Hazard. Mater*. **2008**, 158, 14-22.

29 Kuznetsov, P.N.; Kuznetzova, L.I.; Zhyzhaev, A.M.; Pashkov, G.L.; Boldyrev, V.V. Ultrafast synthesis of metastable tetragonal zirconia by means of mechanochemical activation. *Appl. Catal. A* **2002**, 227, 299-307.

30 Kim, J.; Honma, I. Synthesis and proton conducting properties of zirconia bridged hydrocarbon/phosphotungstic acid hybrid materials. *Electrochim. Acta* **2004**, 49, 3179-3183.

31 Nakamoto, K.; Plenum, P. *Infrared and Raman Spectra of Inorganic and Coordination Compounds*, Wiley: New York; **1978**.

32 Inglezakis, V.J.; Poulopoulos, S.G. *Adsorption, Ion Exchange and Catalysis: Design of Operations and Environmental Applications*, Elsevier: UK; **2006**.

33 Nashaat, N.; Nassar, N. Rapid removal and recovery of Pb(II) from wastewater by magnetic nanoadsorbent, *J. Hazard. Mater*. **2010**, 184, 538-546.

34. Tavakkoli, H.; Hamedi, F. Synthesis of $Gd_{0.5}Sr_{0.5}FeO_3$ perovskite-type nanopowders for adsorptive removal of MB dye from water. *Res. Chem. Intermed*. **2016**, 42, 3005-3027.